Effects of high-temperature ageing on the creep-rupture properties of cobalt-base L-605 alloys

M. TANAKA, H. IIZUKA
Department of Mechanical Engineering for Production, Mining College, Akita University, 1-1, Tegatagakuen-cho, Akita 010, Japan

Effects of high-temperature ageing on the creep-rupture properties of cobalt-base L-605 alloys were investigated at 1089 and 1311 K in air. The specimens with serrated grain boundaries and those with normal straight grain boundaries were aged for 1080 ksec at 1273 or 1323 K to cause the matrix precipitates of tungsten-rich b c c phase and M_6C carbide. The creep-rupture strength of both specimens were improved by the high-temperature ageing. The rupture strength at 1311 K was the highest in the specimens with serrated grain boundaries aged at 1273 K, while the specimens with straight grain boundaries aged at 1273 K of the highest matrix hardness had the highest rupture strength at 1089 K. The high-temperature ageing did not decrease the rupture ductility of specimens. The ruptured specimens with serrated grain boundaries exhibited a ductile grain-boundary fracture surface which consisted of dimple patterns and steps, regardless of whether high-temperature ageing was carried out. The fracture mode of the specimens with straight grain boundaries was changed from the brittle grain-boundary fracture to the ductile one similar to that of the specimens with serrated grain boundaries by high-temperature ageing, since large grain-boundary precipitates which gave nucleation sites of dimples were formed during the ageing. The grain-boundary cracks initiated in the early stage of creep (transient creep regime) in both non-aged and aged specimens of L-605 alloys in creep at 1089 and 1311 K, although the time to crack initiation is shorter in the specimens with straight grain boundaries than in those with serrated grain boundaries. Thus, the period of crack growth and linkage occupied most of the rupture life. The strengthening mechanisms of the aged specimens were also discussed.

1. Introduction

The grain-boundary fracture is the dominant fracture mode in polycrystalline metallic materials at high temperatures. In several heat-resistant alloys, the high-temperature strength can be improved by serrated grain-boundaries accompanied with the carbide precipitation on grain boundaries [1–6]. The serrated grain boundaries are effective in inhibiting the grain-boundary sliding and the subsequent crack initiation on the grain boundaries [1, 3–5, 7]. The crack deflection occurs when a crack propagates on the serrated grain boundaries, and the crack growth rate may be decreased by decrease of the stress intensity factor of the crack [8–10]. The lengthening of crack path due to crack deflection [9], the crack arrest [11], and the occurrence of ductile grain-boundary fracture [4, 5] on the serrated grain boundaries may also be important factors for the strengthening. Further, it has been reported in nickel-base superalloys that the grain-boundary precipitates can retard the creep deformation of the matrix [12].

The present authors [13] have reported that the grain-boundary strengthening is also applicable to low-carbon and high-tungsten cobalt-base L-605 alloys. The serrated grain boundaries are formed by the precipitation of tungsten-rich b c c phase and M_6C carbide in L-605 alloys. Both the rupture life and the rupture ductility of the alloys under low stress and high temperature creep conditions were improved by serrated grain boundaries. But, the strengthening of the matrix is also important for improving the rupture strength of the alloys with serrated grain boundaries [4]. In this study, the effects of high-temperature ageing on the creep-rupture properties are investigated using cobalt-base L-605 alloys at 1089 and 1311 K in air. The strengthening mechanisms in L-605 alloys are then discussed based on the experimental results.

2. Experimental procedure

Cobalt-base L-605 alloys of 20 mm diameter used in the previous study [13] (Table I) were also used in this study. The alloy bars were furnace-cooled and then aged for 72 ksec (20 h) at 1323 K (1050° C) after solution heating for 3.6 ksec (1 h) at 1473 K (1200° C) to obtain specimens with serrated grain boundaries, and were finally water quenched. These specimens are hereafter referred to as specimen S. The specimens

0022-2461/90 $03.00 + .12

TABLE I Chemical composition of cobalt-base L-605 alloys used (wt %)

C	Cr	Ni	W	Mn	Fe	Si	P	S	Co
0.07	19.82	9.83	14.37	1.46	2.22	0.19	< 0.005	0.002	Bal.

with normal straight grain boundaries were obtained by water-quenching after solution heating for 7.2 ksec (2 h) at 1473 K (1200° C) (specimen N). Both specimens have the same grain diameter (about 260 μm). To determine the optimum ageing condition for creep-rupture specimens, disc-like samples of about 5 mm thickness cut out from the round bars were furnace-cooled and then aged for 3.6 to 3.6 $\times$ 10^3 ksec at 1273 or 1323 K after solution heating for 3.6 ksec at 1473 K.

The heat-treated specimens were machined to test pieces of 30 mm gauge length and 5 mm diameter. Creep-rupture tests were performed by using usual tensile creep-rupture equipments at 1089 K (816° C) and 1311 K (1038° C) in air. All the specimens were held for 10.8 ksec (3 h) at each test temperature before application of load. Microstructures of specimens were observed by an optical microscope. Specimens were electrolytically etched by 10% chromic acid in water before observation. Fracture surfaces were examined by a scanning electron microscope. Further, the precipitated phases in specimens were confirmed by dint of X-ray diffraction.

3. Experimental results

3.1. Effects of ageing on microstructures of specimens

Fig. 1 shows the matrix hardness of specimens furnace-cooled and aged at 1273 K (1000° C) or 1323 K (1050° C) after solution heating for 3.6 ksec (1 h) at 1473 K (1200° C). The matrix hardness of specimen gradually increases from about 100 ksec and reaches a value of about 280 Hv over 1000 ksec at 1323 K. The matrix hardness starts to increase from about 40 ksec and becomes more than 300 Hv at 1000 ksec at 1273 K. Thus, the occurrence of the matrix precipitates is earlier and the matrix hardness is higher in the specimen aged at 1273 K than in that aged at 1323 K.

Table II shows the results of X-ray diffraction of the specimens furnace cooled and aged at 1323 K after solution heating for 3.6 ksec at 1473 K. Only grain-boundary precipitates were observed in the specimen aged for 72 ksec (specimen S), while both grain-boundary and matrix precipitates were detected in the specimen aged for 3600 ksec. Weak diffraction peaks of tungsten and very weak diffraction peaks of M_6C carbide were observed in addition to strong diffraction peaks of β-Co matrix phase in both specimens. R. Tanaka and co-workers [12] have reported that

TABLE II Matrix hardness of non-aged and aged specimens

Specimen	No ageing (Hv)	Aged for 1080 ksec at 1273 K (Hv)	Aged for 1080 ksec at 1323 K (Hv)
S	249	301	271
N	253	326	271

Hv: Vickers hardness number (Load 4.9 N)

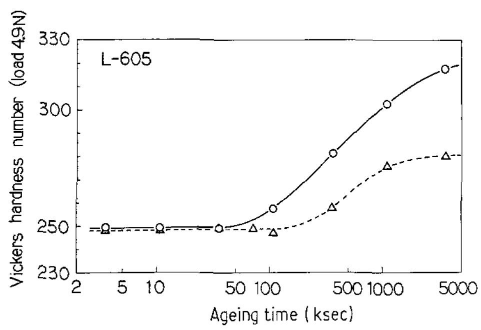

Figure 1 Matrix hardness of specimens furnace-cooled and aged at (○) 1273 or (△) 1323 K after solution heating for 3.6 ksec at 1473 K.

tungsten-rich solid solution (b c c, α_2 phase) precipitated in Ni–20% Cr–20% W superalloys during creep at 1173 and 1273 K. The present authors [13] have also found that tungsten-rich b c c phase and M_6C carbide precipitate on the grain boundary and in the matrix in L-605 alloys during creep at 1311 K (1038° C). Thus, the grain-boundary and matrix precipitates occurred in specimens aged at 1273 and 1323 K are considered to be principally tungsten-rich solid solution accompanied with small amount of M_6C carbide.

According to the experimental results mentioned above, some of specimens with serrated grain boundaries (specimen S) and those with straight grain boundaries (specimen N) for creep-rupture tests were aged for 1080 ksec (300 h) at 1273 or 1323 K. Table III shows the matrix hardness of non-aged specimens and those aged for 1080 ksec at 1273 or 1323 K. In the non-aged condition, specimen S and specimen N have almost the same hardness of about 250 Hv [13] and the matrix hardness of those aged for 1080 ksec at 1323 K is about 270 Hv. The matrix hardness of specimen N (326 Hv) is a little higher than that of specimen S (301 Hv) in ageing at 1273 K.

Fig. 2 shows the microstructures of non-aged and aged specimens for creep-rupture tests. Specimen S has serrated grain boundaries with grain-boundary precipitates of about 5 to 20 μm (Fig. 2a) and specimen N has normal straight grain boundaries (Fig. 2b), but the matrix precipitates are not visible in these specimens. The matrix precipitates can be observed in the aged specimens. The density of matrix precipitates is somewhat high in specimen N (Fig. 2d) compared with specimen S (Fig. 2c) in ageing for 1080 ksec at 1273 K, but it is almost the same in both specimens in ageing for 1080 ksec at 1323 K (Fig. 2e and f). The grain-boundary precipitates are also formed in specimen N aged at 1323 K (about 5 μm in size) (Fig. 2d) and that aged at 1273 K (about 3 μm in size) (Fig. 2f), but the grain boundary is almost straight in these specimens.

3.2. Effect of high-temperature ageing on the creep-rupture properties

Fig. 3 shows the creep-rupture properties of non-aged specimens and those aged for 1080 ksec at 1273 K in creep at 1089 K. The rupture life of specimen S and specimen N largely increases with ageing at 1273 K especially at higher stresses. In non-aged state, the rupture strength of specimen S is almost the same as

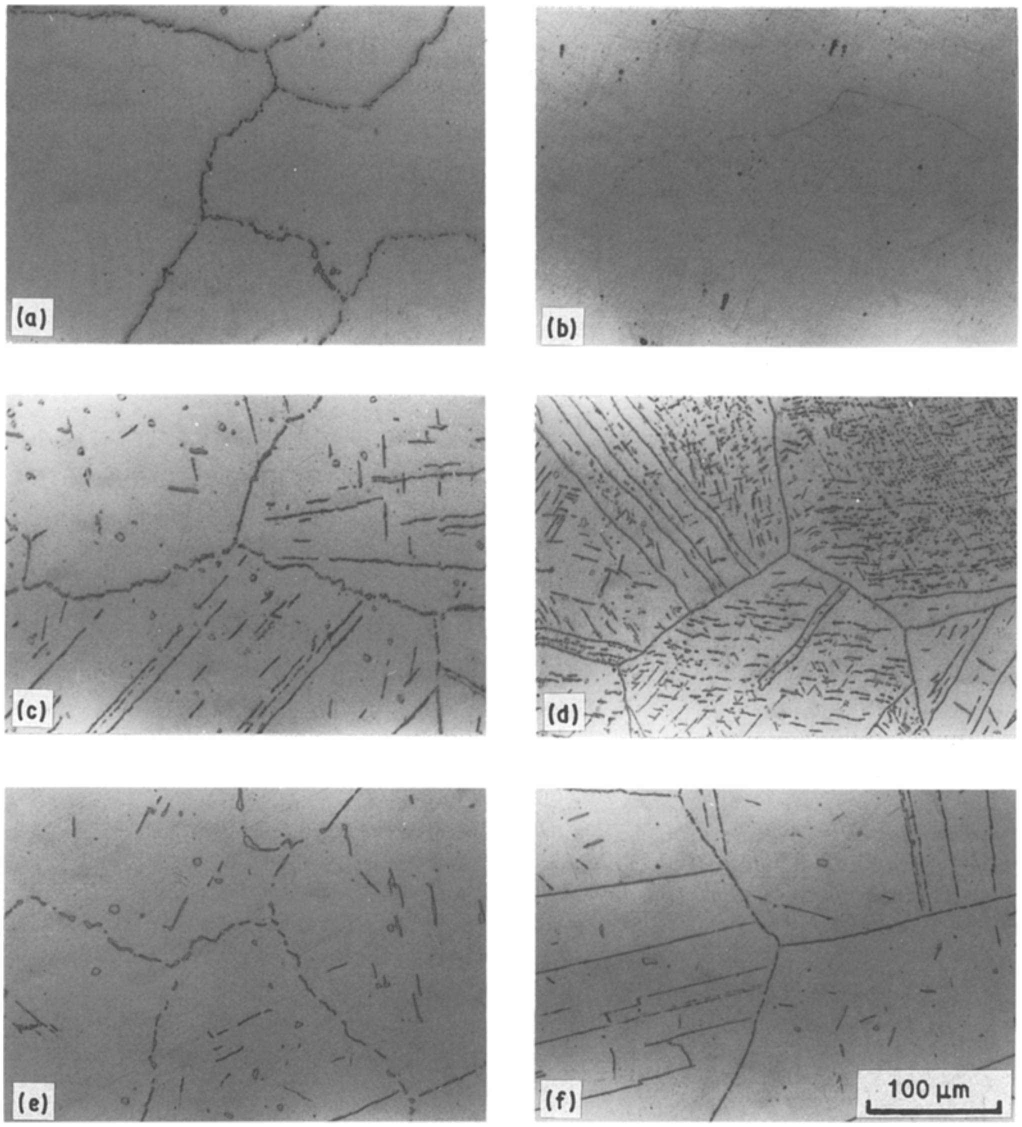

Figure 2 Microstructures of non-aged specimens and those aged for 1080 ksec at 1273 or 1323 K. (a) non-aged specimen S; (b) non-aged specimen N; (c) specimen S aged for 1080 ksec at 1273 K; (d) specimen N aged for 1080 ksec at 1273 K; (e) specimen S aged for 1080 ksec at 1323 K; (f) specimen N aged for 1080 ksec at 1323 K.

that of specimen N [13], but the rupture strength of the aged specimen N of the highest matrix hardness is higher than that of the aged specimen S. Thus, the precipitation hardening of the matrix is effective in increasing the rupture strength of specimens at this temperature. The strength difference between the aged and the non-aged specimens, irrespective of grain-boundary configuration, decreases with decreasing creep stresses, since the precipitation of carbide phases such as M_6C and $M_{23}C_6$ [14–16] which may contribute

TABLE III X-ray diffraction data of specimens furnace-cooled and aged at 1323 K after solution heating for 3.6 ksec at 1473 K.

Specimen aged for 72 ksec		Specimen aged for 3600 ksec		Tungsten (W)*		M_6C*		β-cobalt*	
d_{obs} (nm)	I	d_{obs} (nm)	I	d (nm)	I	d (nm)	I	d (nm)	I
0.2237	w	0.2237	w	0.2238	100				
		0.2223	vw			0.222	80		
0.2067	vs	0.2064	vs			0.2099	100	0.2067	100
0.1924	vw	0.1925	vw			0.1924	80		
0.1790	s	0.1788	s					0.17723	40
0.1581	vw	0.1582	vw	0.1582	15				
		0.1525	vw			0.1521	50		
0.1291	w	0.1291	w	0.1292	23				
0.1283	vw	0.1283	vw			0.1280	80		
0.1266	s	0.1264	s					0.12532	25
		0.08456	vw	0.08459	18				

d_{obs} = observed interplanar spacing; I = relative intensity; w = weak; s = strong; vw = very weak; vs = very strong;
*X-ray diffraction data of ASTM cards.

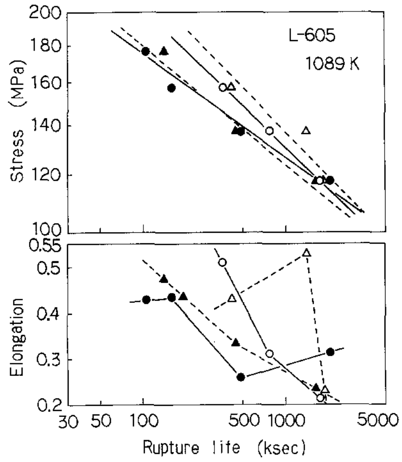

Figure 3 Creep-rupture properties of non-aged specimens (●, ▲) and those aged for 1080 ksec at 1273 K (○, △) in creep at 1089 K. (●, ○) Specimen S; (▲, △) specimen N.

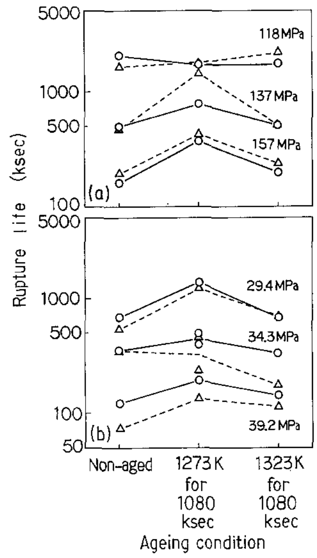

Figure 5 Effects of high-temperature ageing on the rupture life of specimens in creep-rupture tests at (a) 1089 and (b) 1311 K. (○) Specimen S, (△) specimen N.

to precipitation hardening occurs also in the non-aged specimens during creep. The creep-rupture ductility is not decreased by the ageing. The aged specimen N exhibits a little larger elongation compared with the non-aged specimen N.

Fig. 4 shows the properties of non-aged specimens and those aged for 1080 ksec at 1273 K in creep at 1311 K. In both non-aged and aged conditions, specimen S has higher rupture strength and larger ductility than specimen N. High-temperature ageing at 1273 K increases the rupture life of both specimens especially at lower stresses. The rupture ductility of the aged specimen N is larger than that of the non-aged one also at this temperature. Thus, both the strengthening by serrated grain boundaries and the precipitation hardening of matrix are effective at this temperature.

Fig. 5 shows the effects of high-temperature ageing on the rupture life of specimen S and specimen N at 1089 and 1311 K. At 1089 K there is little difference in rupture lives between the non-aged specimens and the specimens aged at 1323 K, probably because the matrix hardness of the specimens aged at 1323 K is not so high (271 Hv) compared with the non-aged specimens (about 250 Hv) (Fig. 2). Ageing at 1273 K largely increases the matrix hardness and improves the rupture life of the specimens under higher stresses at 1089 K. The specimen S with serrated grain boundaries has longer rupture life than the specimen N with straight grain boundaries in both non-aged and aged conditions in creep at 1311 K. The rupture life of the specimen S aged at 1273 K is the longest in all the specimens tested at 1311 K. Thus, ageing at 1273 K is effective in improving rupture lives of specimens.

Fig. 6 shows examples of the creep curves of the non-aged specimens and those aged for 1080 ksec at 1273 K. All the specimens exhibit well-defined metal-type creep curves with transient, steady-state and accelerated creep periods. Creep curves obtained under a stress of 137 MPa at 1089 K shows that ageing for 1080 ksec at 1273 K considerably improves the creep resistance of both specimen S and specimen N without decreasing the rupture ductility. Arrows in the figure indicate the time to crack initiation in those specimens. Cracks in the specimens were nucleated on the grain boundary in the early stage of creep deformation (in transient creep regime). The creep strain to crack initiation was about 0.039 to 0.041 for specimen S and about 0.012 to 0.018 for specimen N in both aged and non-aged conditions.

Fig. 7 shows the effects of ageing for 1080 ksec at 1273 K on the steady-state creep rate of specimens during creep at 1089 and 1311 K. The steady-state

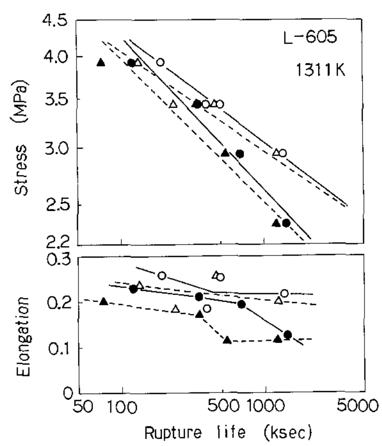

Figure 4 Creep-rupture properties of non-aged specimens (●, ▲) and those aged for 1080 ksec at 1273 K (○, △) in creep at 1311K. (●, ○) Specimen S; (▲, △) specimen N.

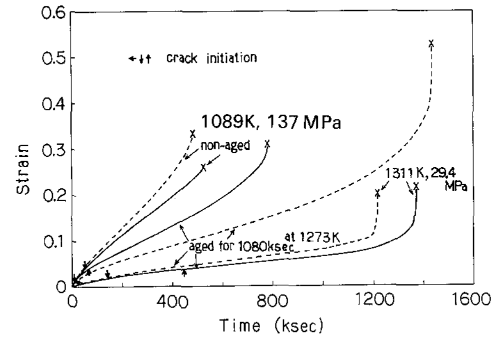

Figure 6 Creep curves of non-aged specimens and those aged for 1080 ksec at 1273 K obtained in creep-rupture tests at 1089 and 1311 K. (——) Specimen S, (- - -) specimen N.

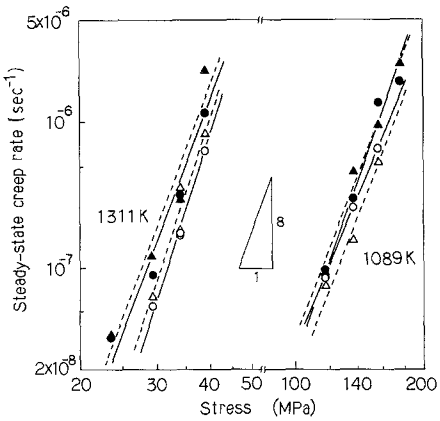

Figure 7 Effects of ageing for 1080 ksec at 1273 K on the steady-state creep rate of specimens during creep at 1089 and 1311 K. Non-aged (●, ▲); aged (○, △). (●, ○) Specimen S; (▲, △) specimen N.

creep rate is almost proportional to the eighth-power of the applied stress in these specimens. The steady-state creep rate of the non-aged specimen N is almost the same as that of the non-aged specimen S at 1089 and 1311 K. Ageing at 1273 K decreases the steady-state creep rate of specimen N more than that of specimen S at 1089 K, since the aged specimen N has higher matrix hardness than the aged specimen S. The steady-state creep rate of specimen S and specimen N at 1311 K is also decreased by the ageing, but there is little difference in the steady-state creep rate between these specimens with different grain-boundary configuration.

3.3. Microstructures and fracture surfaces of ruptured specimens

Fig. 8 shows the microstructures of specimens with or without ageing for 1080 ksec at 1273 K ruptured under a stress of 137 MPa at 1089 K. The tensile direction is horizontal of these photographs. Grain-boundray cracks are visible in both non-aged specimens (Fig. 8a and b) and specimens aged for 1080 ksec at 1273 K (Fig. 8c and d). These grain-boundary cracks are considered to occur at the grain-boundary triple junctions in the primary creep regime (Fig. 6), and the growth and linkage of these cracks lead to the rupture of specimens. Grain boundary precipitates of about 5 to 20 μm are visible in specimen S with or without ageing (Fig. 8a and c). Smaller grain-boundary precipitates (about 3 μm) can be seen in the aged specimen N (Fig. 8d), but those which were formed during creep are very small (less than 1 μm) (Fig. 8b). The fine matrix precipitates can be seen in both the aged and non-aged specimens. The similar grain-boundary cracks were also observed in the specimens aged for 1080 ksec at 1323 K.

Fig. 9 shows the fracture surfaces of the same specimens as those in Fig. 8. The non-aged specimen S exhibits a ductile grain-boundary fracture surface which consists of dimple patterns and steps (Fig. 9a). The size of steps is about 20 μm and corresponds to that of serrated grain-boundary segments (Fig. 8a). This feature of fracture surface is not changed by ageing for 1080 ksec at 1273 K (Fig. 9c). The non-aged specimen N exhibits a brittle grain-boundary fracture surface (Fig. 9b), but the fracture appearance is changed to that of the ductile grain-boundary fracture surface containing dimple patterns similar to those of specimen S by the ageing (Fig. 9d). The ductile grain-boundary fracture also occurred in the specimen N aged for 1080 ksec at 1323 K.

The grain-boundary cracks similar to those observed in the specimens ruptured at 1089 K were also detected

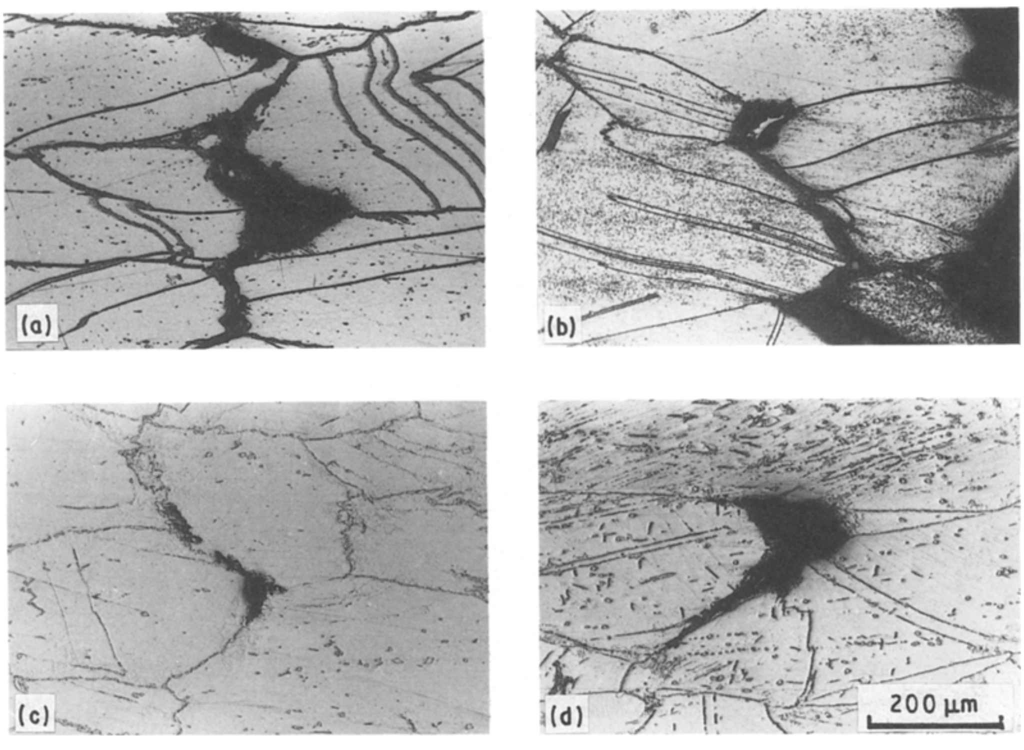

Figure 8 Microstructures of non-aged specimens and those aged for 1080 ksec at 1273 K ruptured under a stress of 137 MPa at 1089 K. (a) non-aged specimen S (t_r = 494 ksec, ε_r = 0.259); (b) non-aged specimen N (t_r = 460 ksec, ε_r = 0.334; (c) aged specimen S (t_r = 780 ksec, ε = 0.311); (d) aged specimen N (t_r = 1438 ksec, ε_r = 0.531), (t_r = rupture life, ε_r = elongation).

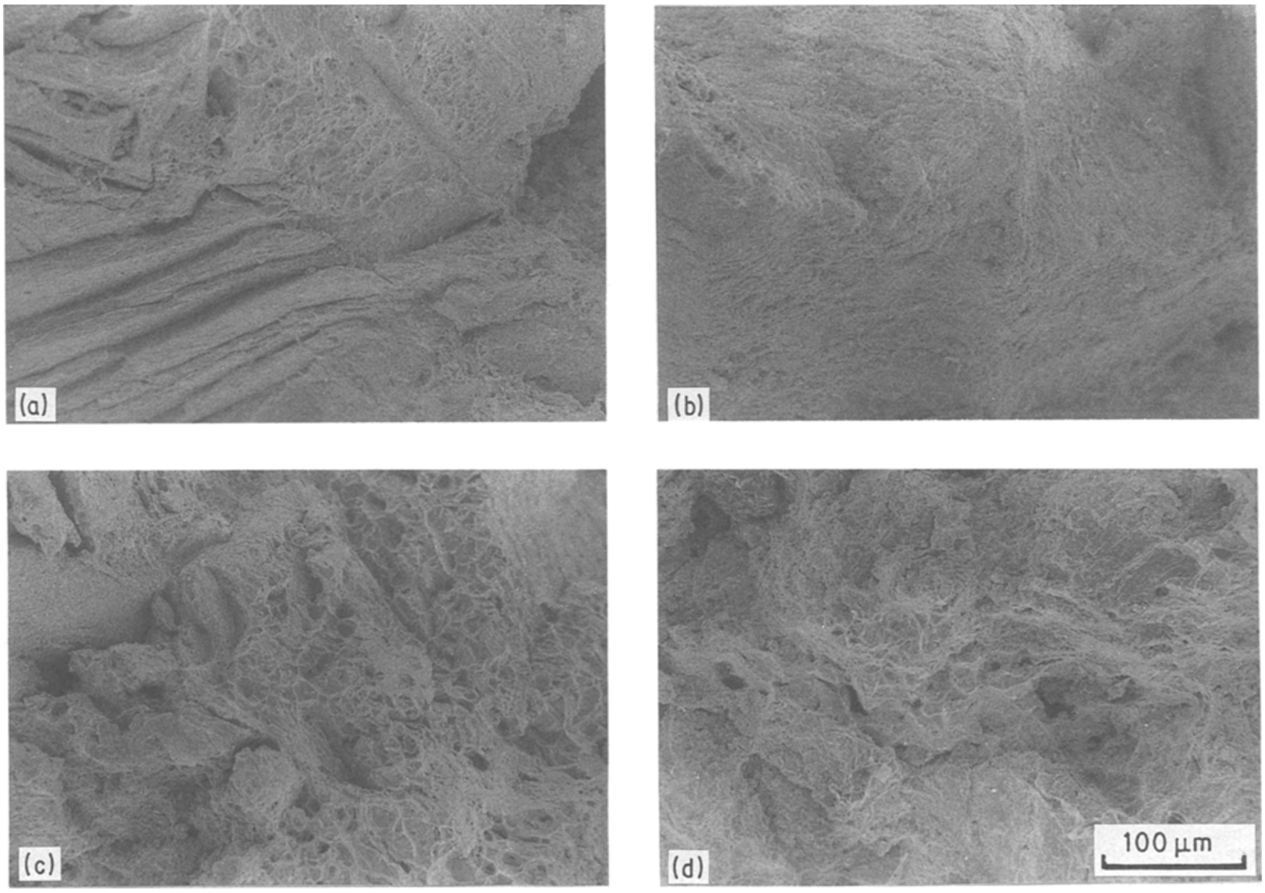

Figure 9 Fracture surfaces of non-aged specimens and those aged for 1080 ksec at 1273 K ruptured under a stress of 137 MPa at 1089 K. (a) non-aged specimen S (t_r = 494 ksec, ε_r = 0.259); (b) non-aged specimen N (t_r = 460 ksec, ε_r = 0.334); (c) aged specimen S (t_r = 780 ksec, ε = 0.311); (d) aged specimen N (t_r = 1438 ksec, ε = 0.531); (t_r = rupture life, ε_r = elongation).

in those ruptured at 1311 K, but the cracks showed finger-like morphology because of enhanced surface diffusion of atoms at this temperature. The fracture appearance of each specimen was not changed with increasing test temperature. Specimen N with high-temperature ageing at 1273 or 1323 K also showed the ductile grain-boundary fracture surface.

4. Discussion

4.1. Effects of grain-boundary and matrix precipitates on the creep-rupture properties

Specimen S has serrated grain boundaries with tungsten-rich b c c phase and M_6C carbide on the grain boundary formed by a heat treatment. It was found in the previous study [13] that both the rupture strength and the rupture ductility of specimen S with serrated grain boundaries is higher than those of specimens with normal straight grain boundaries especially at 1311 K. The strengthening effects of serrated grain boundaries are attributed to the following mechanisms.

1. The inhibition of grain-boundary sliding to retard the initiation of grain-boundary cracks [1, 3–5, 7].
2. The decrease of the stress intensity factor of a crack [8–10] causing the decrease of crack growth rate [17] and the lengthening of crack path [9] when the crack is deflected in propagating on the serrated grain boundaries.
3. The occurrence of ductile grain-boundary fracture on the serrated grain boundaries [4, 5].
4. The crack arrest at the inflection points on the serrated grain boundaries [11].

The time to crack initiation was longer in specimen S with serrated grain boundaries than in specimen N with straight grain boundaries in both aged and non-aged conditions during creep at 1089 and 1311 K, although it was only a small portion of the rupture life of the specimens (Fig. 6). Ductile grain-boundary fracture surfaces composed of dimple patterns and steps were observed in both aged and non-aged specimens with serrated grain boundaries (specimen S) (Fig. 9). These microscopic features are related to the pre-existing grain-boundary precipitates of tungsten-rich b c c phase and M_6C carbide (of about 5 to 20 μm). Therefore, the strengthening by serrated grain boundaries is due to the retardation of growth and linkage of the cracks in L-605 alloys. In this case, the crack deflection (2) and the crack arrest (4) on the serrated grain boundaries, and the occurrence of ductile grain-boundary fracture (3) may be the principal strengthening mechanisms.

The matrix precipitates of tungsten-rich b c c phase and M_6C carbide caused by high-temperature ageing also contribute to the increase of the rupture life of specimen S by increasing the creep strength of the matrix (Figs 3, 4 and 5). The precipitation hardening of the matrix is larger in 1273 K ageing (matrix hardness is 301 Hv) than in 1323 K ageing (matrix hardness is 271 Hv), and the improvement of rupture strength is larger in the former ageing condition (Fig. 5).

Similar grain-boundary precipitates were also formed in specimen N with straight grain boundaries by high-temperature ageing for 1080 ksec at 1273 or 1323 K, but the grain boundaries were almost straight in the aged specimen N as well as the non-aged one (Fig. 2). Therefore, the time to crack initiation of the aged specimen N was also very short and almost the same as that of the non-aged one (Fig. 6).

The high-temperature ageing changed the fracture mechanism of specimen N from the brittle grain-boundary fracture (Fig. 9b) to the ductile grain-boundary fracture (Fig. 9d) composed of dimple patterns similar to those observed on specimen S with serrated grain boundaries. These dimple patterns may be nucleated at the grain-boundary precipitates of tungsten-rich b c c phase and M_6C carbide (of about 3 μm) formed during high-temperature ageing. The increase of the rupture ductility in specimen N by high-temperature ageing is correlated with the change in the fracture mode.

In the aged specimen N as well as specimen S, the crack deflection and the crack arrest on the serrated grain boundaries, and the occurrence of the ductile grain-boundary fracture may be the most important strengthening mechanisms. Further, the growth and linkage of grain-boundary cracks may be considerably decreased by the matrix precipitates of tungsten-rich b c c phase and M_6C carbide caused during high-temperature ageing.

The precipitation of small amounts of $M_{23}C_6$ carbide, Co_2W Laves phase and α-cobalt was also confirmed in the non-aged specimen N ruptured under a stress of 137 MPa at 1089 K [14–16], while only tungsten-rich b c c phase and M_6C carbide were detected in the similar one ruptured under a stress of 29.4 MPa at 1311 K (Table IV). Therefore, it is concluded from the results of creep-rupture tests that the important strengthening phases in L-605 alloy are tungsten-rich b c c phase and M_6C carbide.

TABLE IV X-ray diffraction data of non-aged specimen N after creep rupture at 1089 or 1311 K.

118 MPa, 1089 K t_r = 1645 ksec		29.4 MPa, 1311 K t_r = 540 ksec		Phase*	hkl*
d_{obs} (nm)	I	d_{obs} (nm)	I		
		0.2237	w	W	1 1 0
0.2233	vw			M_6C	4 2 2
0.2174	vw			Co_2W, α–Co	10.3, 10.0
0.2109	w	0.2107	w	M_6C	3 3 3, 5 1 1
0.2065	vs	0.2066	vs	β–Co	1 1 1
0.1978	w			Co_2W	20.1
0.1937	vw			M_6C	4 4 0
0.1789	s	0.1790	s	β–Co	2 0 0
		0.1425	vw	M_6C	5 3 3, 7 3 1
0.1364	vw			Co_2W	30.0
		0.1292	vw	W	2 1 1
0.1289	vw	0.1290	vw	M_6C	6 6 0, 8 2 2
0.1279	vw			α–Co	11.0
0.1265	s	0.1265	s	β–Co	2 2 0
0.1254	vw			$M_{23}C_6$	6 6 0, 8 2 2
0.1229	vw			$M_{23}C_6$	5 5 5, 7 5 1
		0.1100	vw	M_6C	7 5 5, 7 7 1
0.1079	s	0.1079	s	β–Co	3 1 1
		0.08456	vw	W	3 2 1

d_{obs} = observed interplanar spacing; I = relative intensity.
vs = very strong; s = strong; w = weak; vw = very weak; t_r = rupture life.
*X-ray diffraction data of ASTM cards.

4.2. Effects of grain-boundary precipitates on the matrix deformation

It has been reported in nickel-base 20% Cr–20% W superalloy that the grain-boundary precipitation of α_2 phase (tungsten-rich b c c phase) decreases the creep rate and thus increases the creep-rupture strength [12]. If this effect is large in L-605 alloys, the rupture life of the non-aged specimen S with serrated grain boundaries should be always longer than that of the non-aged specimen N with straight grain-boundaries, and the steady-state creep rate should be lower in the former specimen under any creep conditions. The experimental results in this study showed that the rupture life of the non-aged specimen S was not always longer than that of the non-aged specimen N at 1089 K (Fig. 3), and that there is little difference in steady-state creep rate between specimen S and specimen N in the non-aged state under all the test conditions in this study (Fig. 7).

Ageing for 1080 ksec at 1273 or 1323 K caused the precipitation of tungsten-rich b c c phase and M_6C carbide in the matrix of both specimen S and specimen N and also on the grain-boundary of specimen N. If the creep strength of the material is largely affected by grain-boundary precipitates, the steady-state creep rate and the rupture strength of the aged specimen N should be almost the same as the corresponding properties of the aged specimen S. But, the creep-rupture experiments in this study again gave very different results (e.g. Figs 3, 4 and 7). There are still some differences in the creep-rupture properties between those two kinds of specimens even after the high-temperature ageing in creep at 1089 K. The serrated grain boundaries may affect the creep deformation of the matrix near the grain boundary, because the grain-boundary sliding generally involves the deformation of this area [18]. The amount of grain-boundary sliding also increases with increasing test temperature [19]. The grain-boundary sliding is an important factor in the growth of grain-boundary cracks [20–22]. Therefore, the inhibition of grain-boundary sliding by serrated grain boundaries may be more important in creep at 1311 than at 1089 K. This may be one of the reasons that the rupture strength of the specimen S aged for 1080 ksec at 1273 K is higher than that of the specimen N with the same ageing in creep at 1311 K in spite of lower matrix hardness.

5. Conclusions

The effects of high-temperature ageing on the creep-rupture properties were investigated using cobalt-base L-605 alloys at 1089 and 1311 K in air. The results obtained were summarized as follows.

1. The precipitates of tungsten-rich b c c phase and M_6C carbide were formed in the matrix or on the grain boundary during ageing for 1080 ksec at 1273 or 1323 K. The creep-rupture strength of both specimens

with serrated grain boundaries and those with straight grain boundaries increased with high-temperature ageing without decreasing the rupture ductility. The rupture strength at 1311 K was the highest in the specimens with serrated grain boundaries aged at 1273 K, while the specimens with straight grain boundaries aged at 1273 K of the highest matrix hardness had the longest rupture life at 1089 K. Ageing at 1273 K was more effective in improving the rupture strength than ageing at 1323 K, since the precipitation hardening of the matrix was larger in the former ageing.

2. The fracture surface of the specimens with serrated grain boundaries was a ductile grain-boundary fracture surface which consisted of dimple patterns and steps corresponding to serrated grain boundaries, regardless of with or without high-temperature ageing. The fracture mode of the specimens with straight grain boundaries was changed from the brittle grain-boundary fracture to the ductile one similar to that observed in the specimens with serrated grain boundaries, since the grain-boundary precipitates caused by high-temperature ageing became nucleation sites of dimple patterns. The rupture ductility of these specimens also increased with the change in the fracture mode.

3. The grain-boundary cracks initiated in the early stage of creep (transient creep regime) in both non-aged specimens in creep at 1089 and 1311 K, although the time to crack initiation was shorter in the specimens with straight grain boundaries than in the specimens with serrated grain boundaries. Therefore, the growth and linkage of the grain-boundary cracks occupied most of the rupture life of these specimens.

4. The strengthening effects of grain-boundary precipitates were attributed to the crack deflection and the crack arrest on the serrated grain boundaries, and the occurrence of the ductile grain-boundary fracture. The similar strengthening mechanisms also worked in the aged specimens with straight grain boundaries. The serrated grain boundaries had little effect on the creep deformation, since this effect was restricted to the matrix near grain boundaries.

Acknowledgements
The authors thank Mr H. Mitobe for his assistance in experiments. Mitubishi Metal Company is acknowledged for providing the material.

References
1. M. YAMAZAKI, *J. Jpn Inst. Met.* **30** (1966) 1032.
2. H. KLEMM, *Metall.* **63** (1963) 113.
3. M. KOBAYASHI, M. YAMAMOTO, O. MIYAGAWA, T. SAGA and D. FUJISHIRO, *Tetsu to Hagané,* **58** (1972) 859.
4. M. YAMAMOTO, O. MIYAGAWA, M. KOBAYASHI and D. FUJISHIRO, *ibid.* **63** (1977) 1848.
5. M. TANAKA, O. MIYAGAWA, T. SAKAKI and D. FUJISHIRO, *ibid.* **65** (1979) 939.
6. M. TANAKA, H. IIZUKA and F. ASHIHARA, *J. Mater. Sci.* **24** (1989) 1623.
7. M. TANAKA, O. MIYAGAWA, T. SAKAKI, H. IIZUKA, F. ASHIHARA and D. FUJISHIRO, *ibid.* **23** (1988) 621.
8. H. KITAGAWA and R. YUUKI, *Trans Jpn Soc. Mech. Eng.* **41** (346) (1975) 1641.
9. S. SURESH, *Metall. Trans.* **14A** (1983) 2375.
10. M. ISHIDA, *Trans. Jpn Soc. Mech. Eng.* **45** (392) (1979) 306.
11. R. OHTANI, M. OKUNO and R. SHIMIZU, *J. Soc. Mater. Sci. Jpn* **31** (344) (1982) 505.
12. R. TANAKA, M. KIKUCHI, T. MATSUO, S. TAKEDA, N. NISHIKAWA, T. ICHIHARA and M. KAJIHARA, Proceedings of the Fourth International Symposium on Superalloys, edited by J. K. Tien, S. T. Wlodek, H. Morrow III, M. Gel and G. E. Maurer, 1980 (American Society of Metals, Metals Park, Ohio, 1980) p. 481.
13. M. TANAKA, H. IIZUKA and M. TAGAMI, *J. Mater. Sci.* **24** (1989) 2421.
14. S. T. WLODEK, *Trans. ASM* **56** (1963) 287.
15. G. D. SANDROCK and L. LEONARD, NASA TN D-3528.
16. N. YUKAWA and K. SATO, *Trans. Jpn Inst. Metals* **9** (1968) 680.
17. M. TANAKA, H. IIZUKA and F. ASHIHARA, *J. Mater. Sci.* **23** (1988) 3827.
18. T. WATANABE, *Bull. Jpn Inst. Metals* **12** (1973) 883.
19. E. HORNBOGEN, "Festigkeits- und Bruchverhalten bei höheren Temperaturen," **1** (Verlag Stahleisen M. B. H., Düsseldorf, 1980) p. 31.
20. D. McLEAN, *J. Inst. Metals* **85** (1956–57) 468.
21. J. A. WILLIAMS, *Acta Metall.* **15** (1967) 1119.
22. T. G. LANGDON, *Phil. Mag.* **23** (1970) 945.

Received 4 July
and accepted 12 December 1989